

周期场驱动双通道四波混频的竞争与控制

李院院*

西京学院信息工程学院, 陕西 西安 710123

摘要 采用密度矩阵方程,分析了倒 Y 四能级原子系统中相位周期场驱动的双通道四波混频(FWM)过程。数值分析结果表明:周期性相位调制的探测场可以调控两个通道的 FWM 信号,使之叠加或分离;选择不同的调制频率、调制系数及缀饰场强度,可使 FWM 信号出现抑制、增强或分裂。这种周期场驱动的调控方法有望用于光学非线性过程的优化及光信息处理。

关键词 非线性光学; 四波混频; 周期相位调制; 缀饰效应; 电磁诱导透明

中图分类号 O433 文献标识码 A

doi: 10.3788/LOP56.121901

Competition and Control of Two Four-Wave Mixing Processes Driven by Periodic Field

Li Yuanyuan*

School of Information Engineering, Xijing University, Xi'an, Shaanxi 710123, China

Abstract This study investigates the four-wave mixing (FWM) processes from two channels in an inverted Y-type four-level atomic system driven by a periodic phase-modulation field using the density matrix equation. The numerical analysis results denote that the FWM signals from the two channels can be controlled to overlap or separate by the probe field with periodic phase modulation. The suppression, enhancement, and splitting of the FWM signals can be observed by selecting different modulation frequencies, modulation coefficients, and dressing field strengths. This FWM control with a periodically driven field can be probably used in the optimization of optical nonlinear processes and the optical information processing.

Key words nonlinear optics; four-wave mixing; periodic phase modulation; dressing effect; electromagnetically induced transparency

OCIS codes 190.4380; 190.4223; 270.1670

1 引言

早在 1990 年, Harris 等^[1]从理论上预言强耦合场作用下电磁诱导透明(EIT)与增强的三阶非线性过程可同时发生,从而能极大地提高四波混频(FWM)的转换效率。随后, Zhang 等^[2]于 1993 年实验证实了这一理论。自此, EIT 辅助的 FWM 过程得到了极大关注和深入研究^[3-13]。通过改变四能级系统的色散特征,之前不存在的 FWM 过程可以出现并得到极大程度地增强^[3]。在一个基于 EIT 的五能级系统中,双光子及三光子吸收均被有效抑制, FWM 信号的幅度可增加几个量级^[4]。双重暗

态可以显著改变吸收及色散特性,并得到高效的 FWM 信号,通过改变耦合场的强度可实现对 FWM 信号的有效控制^[5-6]。改变缀饰场的强度可使 FWM 信号得到增强或抑制^[7-10],从而实现对 FWM 的相干控制^[11]。最近的研究发现,通过 EIT 条件下的相干控制,转换效率达 63% 的 FWM 过程得以在冷原子系统中实现^[12]。此外,改变驱动场的相对相位可以有效控制 EIT 条件下的克尔非线性系数^[13]。可控 FWM 在量子信息处理等领域具有重要的应用前景,例如借助 FWM,可将近红外抽运光所包含的轨道角动量信息完全传递至蓝色的产生光^[14],可实现光子与存储器的非对称角动量接口^[15]、频率上转

收稿日期: 2018-11-23; 修回日期: 2019-01-06; 录用日期: 2019-01-09

* E-mail: liyynxcn@aliyun.com

换及下转换参量过程中轨道角动量的加减及擦除运算^[16]、光涡旋变换^[17]、单光子源^[18]及双光子源^[19]的产生,以及FWM非线性过程的优化^[20]等。

在FWM的缀饰调控中,通常需要外加不参与FWM过程的缀饰场来控制FWM信号,其缀饰机制较为清晰。而参与FWM过程的耦合场内缀饰效应还有待进一步研究。本文采用单束周期性相位调制的探测场同时驱动两个FWM过程,研究在相位调制场及内缀饰场的共同作用下,两个FWM过程的竞争与控制。

2 理 论

原子能级结构及光束配置如图1所示,其中 $|0\rangle$ 、 $|3\rangle$ 对应原子基态的两个超精细能级, $|1\rangle$ 、 $|2\rangle$

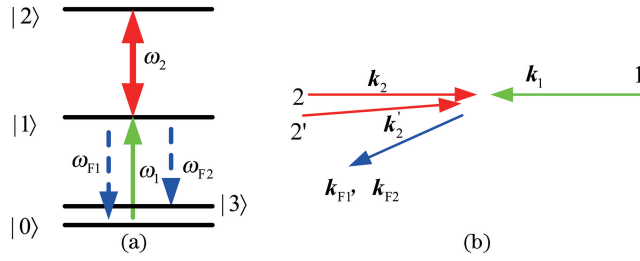


图1 光束配置示意图。(a)原子能级结构;(b)光束配置

Fig. 1 Diagram of beam configuration. (a) Energy-level structure; (b) beam configuration

FWM1及FWM2分别正比于密度矩阵元 $\sigma_{10}^{(3)}$ 及 $\sigma_{13}^{(3)}$ 的模的平方。根据光场与原子相互作用的物理机制,假定探测光对应FWM1及FWM2通道的Rabi频率 $g_3=g_1$,耦合场的Rabi频率 $g_2=g'_2$,密度矩阵方程可表示为

$$\begin{aligned} \partial\sigma_{10}^{(3)}/\partial t = & -\Lambda_{10}\sigma_{10}^{(3)} + \\ & ig_1[\sigma_{00}^{(2)} - \sigma_{11}^{(2)}] + ig_2\sigma_{20}^{(2)} + ig_1\sigma_{30}^{(2)}, \end{aligned} \quad (1)$$

$$\begin{aligned} \partial\sigma_{13}^{(3)}/\partial t = & -\Lambda_{13}\sigma_{13}^{(3)} + \\ & ig_1[\sigma_{33}^{(2)} - \sigma_{11}^{(2)}] + ig_2\sigma_{23}^{(2)} + ig_1\sigma_{03}^{(2)}, \end{aligned} \quad (2)$$

$$\begin{aligned} \partial\sigma_{00}^{(2)}/\partial t = & -ig_1[\sigma_{01}^{(1)} - \sigma_{10}^{(1)}] + \\ & \gamma_{10}\sigma_{11}^{(2)} + \gamma_{30}\sigma_{33}^{(2)} - \gamma_{30}\sigma_{00}^{(2)}, \end{aligned} \quad (3)$$

$$\begin{aligned} \partial\sigma_{11}^{(2)}/\partial t = & ig_1[\sigma_{01}^{(1)} - \sigma_{10}^{(1)}] + ig_2[\sigma_{21}^{(1)} - \sigma_{12}^{(1)}] + \\ & ig_3[\sigma_{31}^{(1)} - \sigma_{13}^{(1)}] + \gamma_{21}\sigma_{22}^{(2)} - \Gamma_1\sigma_{11}^{(2)}, \end{aligned} \quad (4)$$

$$\begin{aligned} \partial\sigma_{20,23}^{(2)}/\partial t = & -\Lambda_{20,23}\sigma_{20,23}^{(2)} + ig_2\sigma_{10,13}^{(1)} - ig_{1,3}\sigma_{21}^{(1)}, \end{aligned} \quad (5)$$

$$\begin{aligned} \partial\sigma_{30,03}^{(2)}/\partial t = & -\Lambda_{30,03}\sigma_{30,03}^{(2)} \pm ig_1\sigma_{10,01}^{(1)} \mp ig_1\sigma_{31,13}^{(1)}, \end{aligned} \quad (6)$$

$$\begin{aligned} \partial\sigma_{33}^{(2)}/\partial t = & ig_1[\sigma_{13}^{(1)} - \sigma_{31}^{(1)}] + \\ & \gamma_{13}\sigma_{11}^{(2)} - \gamma_{30}\sigma_{33}^{(2)} + \gamma_{30}\sigma_{00}^{(2)}, \end{aligned} \quad (7)$$

$$\partial\sigma_{22}^{(2)}/\partial t = ig_2[\sigma_{12}^{(1)} - \sigma_{21}^{(1)}] - \gamma_{21}\sigma_{22}^{(2)}, \quad (8)$$

$$\partial\sigma_{10,01}^{(1)}/\partial t = -\Lambda_{10,01}\sigma_{10,01}^{(1)} \pm$$

$$ig_1[\sigma_{00}^{(0)} - \sigma_{11}^{(0)}] \pm ig_2\sigma_{20,02}^{(0)} \pm ig_1\sigma_{30,03}^{(0)}, \quad (9)$$

分别为原子中间态及激发态。 $|0\rangle \rightarrow |1\rangle$ 、 $|3\rangle \rightarrow |1\rangle$ 及 $|1\rangle \rightarrow |2\rangle$ 对应的跃迁频率分别为 Ω_1 、 Ω_2 及 Ω_3 。光束1为探测场 $\epsilon_1(t) = \epsilon_{10} \exp\{-i[\omega_1 t + \varphi(t) + \mathbf{k}_1 \cdot \mathbf{r}]\}$,其中 ϵ_{10} 为场振幅, \mathbf{r} 为位置矢量, ω_1 为角频率, \mathbf{k}_1 为波矢量, $\varphi(t) = A \sin(\nu t)$ 为相位调制函数, A 与 ν 分别为调制系数及调制频率, t 为时间。显然探测场是非单色光,可以同时激发 $|0\rangle \rightarrow |1\rangle$ 及 $|3\rangle \rightarrow |1\rangle$ 的跃迁。光束2及2'为耦合场 ϵ_2 及 ϵ'_2 (频率为 ω_2 ,波矢为 \mathbf{k}_2 及 \mathbf{k}'_2),其间有非常小的夹角约为 0.5° ,对应于 $|1\rangle \rightarrow |2\rangle$ 的跃迁。当满足相位匹配条件 $\mathbf{k}_{F1,F2} = \mathbf{k}_1 + \mathbf{k}_2 - \mathbf{k}'_2$ 时,光束2'几乎沿反方向传输,波矢量分别为 \mathbf{k}_{F1} 及 \mathbf{k}_{F2} 的两个FWM信号FWM1及FWM2可同时产生。

$$\begin{aligned} \partial\sigma_{21,12}^{(1)}/\partial t = & -\Lambda_{21,12}\sigma_{21,12}^{(1)} \mp \\ & ig_1\sigma_{20,02}^{(0)} \mp ig_2[\sigma_{22}^{(0)} - \sigma_{11}^{(0)}] \mp ig_1\sigma_{23,32}^{(0)}, \end{aligned} \quad (10)$$

$$\begin{aligned} \partial\sigma_{13,31}^{(1)}/\partial t = & -\Lambda_{13,31}\sigma_{13,31}^{(1)} \pm \\ & ig_1[\sigma_{33}^{(0)} - \sigma_{11}^{(0)}] \pm ig_2\sigma_{23,32}^{(0)} \pm ig_1\sigma_{03,30}^{(0)}, \end{aligned} \quad (11)$$

式中: $\sigma^{(m)}$ 为 m 阶密度矩阵元($m=0,1,2,3$);复失谐量 $\Lambda_{10} = \gamma_{10} - i[\Delta_1 + \varphi'(t)]$, $\Lambda_{13} = \gamma_{13} - i[\Delta_3 + \varphi'(t)]$, $\Lambda_{20} = \gamma_{20} - i[\Delta_1 + \Delta_2 + \varphi'(t)]$, $\Lambda_{23} = \gamma_{23} - i[\Delta_3 + \Delta_2 + \varphi'(t)]$, $\varphi'(t)$ 为相位调制函数关于 t 的一阶导数; $\Lambda_{30} = \gamma_{30} - i\Delta$, $\Lambda_{21} = \gamma_{21} - i\Delta_2$, $\Lambda_{ij} = \Lambda_{ji}^*$ (能级序号 $i, j=0,1,2,3, i \neq j$),其中失谐量 $\Delta_j = \omega_j - \Omega_j$ ($j=1,2,3$); Δ 为两个超精细能级 $|0\rangle$ 及 $|3\rangle$ 间的分裂差; $\gamma_{ij} = \gamma_{ji} = (\Gamma_i + \Gamma_j)/2$ ($i, j=0,1,2,3, i \neq j$),其中 Γ_i (Γ_j)为 $|i\rangle$ ($|j\rangle$)的衰变率。

为简化计算,假定原子初始布居于 $|0\rangle$ 能级,即 $\sigma_{00}^{(0)} = 1$,则可得 $\sigma_{ij}^{(0)} = 0$ ($i = j = 1, 2, 3$)及 $\sigma_{12,21}^{(1)} = \sigma_{13,31}^{(1)} = \sigma_{22}^{(2)} = \sigma_{23}^{(2)} = 0$ 。此外,上述密度矩阵方程中(2)、(4)~(7)及(9)式可分别简化为

$$\partial\sigma_{13}^{(3)}/\partial t = -\Lambda_{13}\sigma_{13}^{(3)} + ig_1[\sigma_{33}^{(2)} - \sigma_{11}^{(2)}] + ig_1\sigma_{03}^{(2)}, \quad (12)$$

$$\partial\sigma_{11}^{(2)}/\partial t = ig_1[\sigma_{01}^{(1)} - \sigma_{10}^{(1)}] - \Gamma_1\sigma_{11}^{(2)}, \quad (13)$$

$$\partial\sigma_{20}^{(2)}/\partial t = -\Lambda_{20}\sigma_{20}^{(2)} + ig_2\sigma_{10}^{(1)}, \quad (14)$$

$$\partial\sigma_{30}^{(2)}/\partial t = -\Lambda_{30}\sigma_{30}^{(2)} + ig_1\sigma_{10}^{(1)}, \quad (15)$$

$$\partial\sigma_{33}^{(2)}/\partial t = \gamma_{13}\sigma_{11}^{(2)} - \gamma_{30}\sigma_{33}^{(2)} + \gamma_{30}\sigma_{00}^{(2)}, \quad (16)$$

$$\partial\sigma_{10,01}^{(1)}/\partial t = -\Lambda_{10,01}\sigma_{10,01}^{(1)} \pm ig_1. \quad (17)$$

由(1)式及(12)式可知,FWM1过程取决于布居差 $\Delta\sigma_1 = \sigma_{00}^{(2)} - \sigma_{11}^{(2)}$ 和双光子相干项 $\sigma_{20}^{(2)}$ 及 $\sigma_{30}^{(2)}$ 的竞争与演化;而FWM2过程取决于布居差 $\Delta\sigma_2 = \sigma_{33}^{(2)} - \sigma_{11}^{(2)}$ 及双光子相干项 $\sigma_{03}^{(2)}$ 的竞争与演化。这种演化会导致两个通道FWM过程的分离、增强或抑制。此外,FWM1明显受内缀饰场 $g_2(g'_2)$ 的调控。相反,缀饰场对FWM2的调控作用则可以忽略。

3 数值结果及讨论

可以采用传统的傅里叶变换求解上述密度矩阵方程,得到对应能级跃迁的场分量,再分析相关信号的演化。但这种方法求解过程繁琐,且不完备。采用与文献[21]相近的方法求 $\sigma_{10}^{(3)}$ 及 $\sigma_{13}^{(3)}$ 的数值解,并得到其对应的FWM信号。

以 ^{85}Rb 原子的 $5S_{1/2}(F=2)$ 、 $5S_{1/2}(F=3)$ 、 $5P_{1/2}$ 及 $5D_{1/2}$ 为例,选择 $\gamma_{10,13} = 2\pi \times 3\text{ MHz}$ 、 $\gamma_{21} = 2\pi \times 0.8\text{ MHz}$ 、 $\gamma_{30} = 2\pi \times 1\text{ kHz}$ 、 $\gamma_{20,23} = 0$ 及 $\Gamma_1 = 2\pi \times 6\text{ MHz}$ 。假定探测场很弱,其Rabi频率为 $g_1 = g_3 = 0.01\gamma_{10}$;缀饰场的强度远大于探测场的强度,且精确调谐于能级 $|1\rangle \rightarrow |2\rangle$ 的跃迁,则其失谐量 $\Delta_2 = 0$ 。由于 $\Delta_3 = \Delta_1 - \Delta$,下文仅讨论失谐量 Δ_1 变化时的情形。此外, λ 三能级系统 $|0\rangle \rightarrow |1\rangle \rightarrow |3\rangle$ 中,典型的调制频率 $\nu = \Delta/n$ (n 为正整数)时可出现暗态,因此本文限于讨论 ν 在 $\Delta/2$ 附近及 $\Delta/10 < \nu < \Delta/2$ 时FWM信号的演化情况。

图2(a)、(b)、(c)分别为探测光的失谐量 $\Delta_1/\Delta = 0.25, 0.50, 0.75$ 时FWM1及FWM2信号对应的谱线,其中缀饰场的Rabi频率 $g_2 = g'_2 = 0.3\gamma_{10}$ 。可以发现,当 $\Delta_1/\Delta = 0.50$ 时,两个FWM信号可以叠加;而当 $\Delta_1/\Delta = 0.25$ 和 0.75 时FWM1及FWM2分别出现在频率 $\nu = \Delta_1$ 和 $\Delta - \Delta_1$ 的位置,实现了两个信号的分离。失谐量(调制频率)较小时,无论是FWM1还是FWM2均可得到增强;而当失谐量(调制频率)增大时,FWM信号被抑制。这种增强或抑制对应原子处于共振或偏离共振区域时FWM信号的增大或减小。

在缀饰场相对较弱时($g_2 = g'_2 = 0.3\gamma_{10}$),固定探测场的失谐量 $\Delta_1/\Delta = 0.50$,改变调制系数 A 可多样化地增强或抑制FWM峰,如图3所示。当 $A \leq 1$ 时, $\nu = \Delta_1$ 处FWM信号的幅度远远大于低频区的信号强度,由于缀饰强度较弱,此时 λ 三能级 $|0\rangle \rightarrow |1\rangle \rightarrow |3\rangle$ 的相干布居囚禁(CPT)起主导

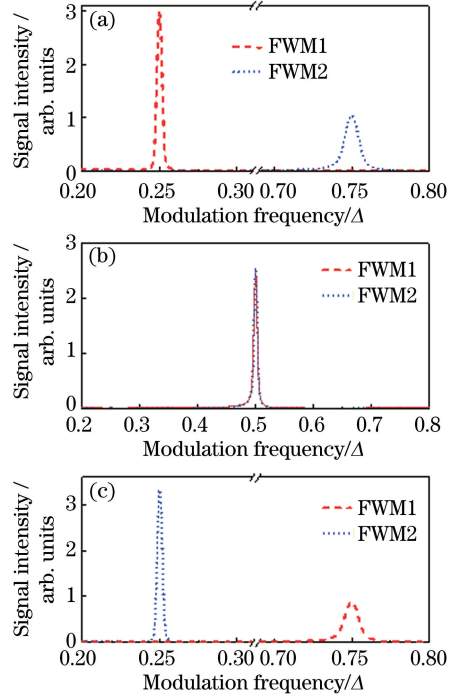


图2 $g_2 = g'_2 = 0.3\gamma_{10}$ 时不同 Δ_1 对应的FWM谱线。

(a) $\Delta_1/\Delta = 0.25$; (b) $\Delta_1/\Delta = 0.50$; (c) $\Delta_1/\Delta = 0.75$

Fig. 2 FWM lines at different Δ_1 for $g_2 = g'_2 = 0.3\gamma_{10}$.

(a) $\Delta_1/\Delta = 0.25$; (b) $\Delta_1/\Delta = 0.50$; (c) $\Delta_1/\Delta = 0.75$

作用,因而FWM2的峰值略大于FWM1。而当 $A > 1$ 时, $\nu = \Delta_1$ 处FWM信号的幅度则极大减弱。在调制频率低频区,CPT效应主要出现在 $\nu = \Delta/n$ ($n \geq 3, n$ 为正整数)处,其对应的FWM信号随调制系数的增大而得到极大增强。此时 $|0\rangle \rightarrow |1\rangle \rightarrow |2\rangle$ 级联三能级系统的EIT效应较为显著,FWM1信号的峰值略大于FWM2。由于内缀饰效应产生相消干涉,部分FWM1信号出现了Autler Townes(AT)分裂。

图4为改变缀饰场强度时FWM信号的演化情况,其中调制系数为 $A = 1$ 。可以发现,随着缀饰场强度的增大,在 $\Delta_1/\Delta = 0.25$ 及 0.05 处,FWM1信号峰开始被抑制,并逐渐出现了AT分裂。由于 $|3\rangle \rightarrow |1\rangle \rightarrow |2\rangle$ 级联三能级系统的量子相干效应可以忽略,FWM1的抑制和分裂主要是 λ 三能级系统的布居差 $\Delta\sigma_1 = \sigma_{00}^{(2)} - \sigma_{11}^{(2)}$ (CPT)与 $|0\rangle \rightarrow |1\rangle \rightarrow |2\rangle$ 级联三能级系统EIT效应相关的原子相干项 $\sigma_{20}^{(2)}$ 竞争的结果。显然,缀饰场强度越大,原子相干效应越显著,此时FWM1主要由 $\sigma_{20}^{(2)}$ 主导。由图4可知,当其他参数保持不变时,FWM2信号几乎不受缀饰场的调控,这一点在前面理论部分已有所述。

在强缀饰场的作用下(以 $g_2 = g'_2 = 3\gamma_{10}$ 为例),

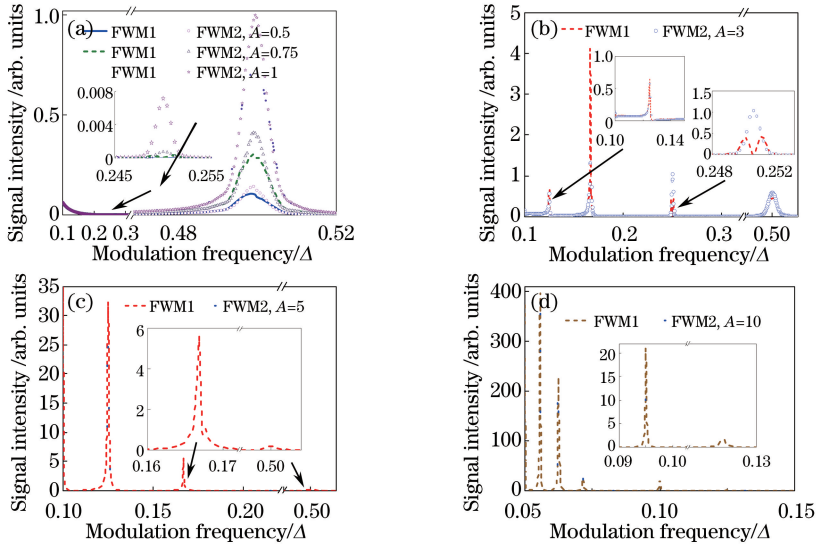


图 3 $g_2 = g_2' = 0.3\gamma_{10}$ 时对应不同调制系数的 FWM 谱线。(a) $A = 0.5, 0.75, 1$; (b) $A = 3$; (c) $A = 5$; (d) $A = 10$
 Fig. 3 FWM lines at different modulation coefficients for $g_2 = g_2' = 0.3\gamma_{10}$. (a) $A = 0.5, 0.75, 1$; (b) $A = 3$; (c) $A = 5$; (d) $A = 10$

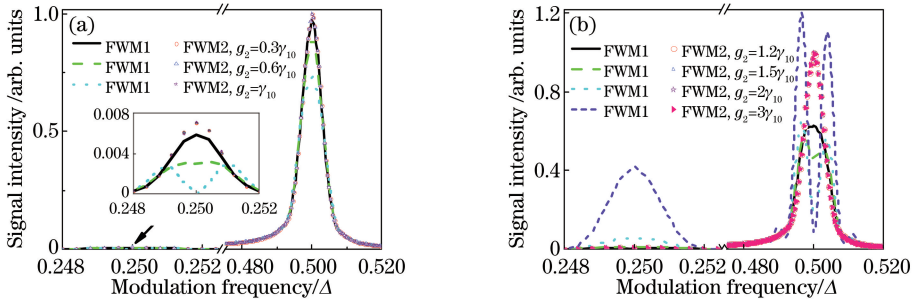


图 4 不同缀饰场强度对应的 FWM 谱线。(a) $g_2/\gamma_{10} = 0.3, 0.6, 1$; (b) $g_2/\gamma_{10} = 1.2, 1.5, 2, 3$
 Fig. 4 FWM lines at different dressing field strengths. (a) $g_2/\gamma_{10} = 0.3, 0.6, 1$; (b) $g_2/\gamma_{10} = 1.2, 1.5, 2, 3$

探测光的调制系数亦可对 FWM 信号进行有效调控。由图 5 可知,对 FWM1 信号而言,调制系数可以显著改变其分裂深度及分裂峰的强度。而对 FWM2 信号,虽然不会出现类似 FWM1 的 AT 分裂,但仍可显著改变信号的峰值强度。

4 结 论

以倒 Y 四能级原子系统为例,考虑两束强耦合光与一束周期性相位调制的探测光共同作用于系统时对应两个通道 FWM 信号的竞争与调控机制。通过对密度矩阵方程数值求解,发现周期性调制的探测场可以调控两个通道的 FWM 信号,使之叠加或分离;选择不同调制频率、调制系数及内缀饰场强度可使 FWM 信号出现抑制、增强或分裂。这种竞争与演化对 FWM1 过程而言,主要取决于布居差 $\Delta\sigma_1 = \sigma_{00}^{(2)} - \sigma_{11}^{(2)}$ (CPT) 与双光子相干项 $\sigma_{20}^{(2)}$ (EIT) 竞

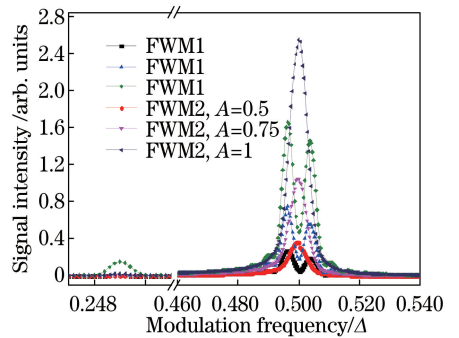


图 5 强缀饰场作用时不同调制指数对应的 FWM 谱线
 Fig. 5 FWM lines at different modulation coefficients under action of strong dressing field

争的结果;而对于 FWM2 过程则取决于布居差 $\Delta\sigma_2 = \sigma_{33}^{(2)} - \sigma_{11}^{(2)}$ (CPT) 的演化。研究结果可望用于光学非线性过程的优化及光信息处理。

参 考 文 献

- [1] Harris S E, Field J E, Imamoglu A. Nonlinear optical processes using electromagnetically induced transparency[J]. Physical Review Letters, 1990, 64(10): 1107-1110.
- [2] Zhang G Z, Hakuta K, Stoicheff B P. Nonlinear optical generation using electromagnetically induced transparency in atomic hydrogen[J]. Physical Review Letters, 1993, 71(19): 3099-3102.
- [3] Deng L, Kozuma M, Hagley E W, *et al.* Opening optical four-wave mixing channels with giant enhancement using ultraslow pump waves [J]. Physical Review Letters, 2002, 88(14): 143902.
- [4] Wu Y, Saldana J, Zhu Y F. Large enhancement of four-wave mixing by suppression of photon absorption from electromagnetically induced transparency[J]. Physical Review A, 2003, 67(1): 013811.
- [5] Niu Y P, Li R X, Gong S Q. High efficiency four-wave mixing induced by double-dark resonances in a five-level tripod system [J]. Physical Review A, 2005, 71(4): 043819.
- [6] Li H J, Huang G X. Highly efficient four-wave mixing in a coherent six-level system in ultraslow propagation regime[J]. Physical Review A, 2007, 76(4): 043809.
- [7] Zhang Y P, Brown A W, Xiao M. Opening four-wave mixing and six-wave mixing channels via dual electromagnetically induced transparency windows [J]. Physical Review Letters, 2007, 99(12): 123603.
- [8] Li Y, Li L, Zhang Y. Intensity dependence suppression and enhancement of four-wave mixing in a micrometric thin vapour [J]. Journal of Modern Optics, 2010, 57(10): 885-892.
- [9] Li Y Y, Huang G P, Zhang D, *et al.* Density control of dressed four-wave mixing and super-fluorescence [J]. IEEE Journal of Quantum Electronics, 2014, 50(1): 25-34.
- [10] Zhang Z Y, Wen F, Che J L, *et al.* Dressed gain from the parametrically amplified four-wave mixing process in an atomic vapor [J]. Scientific Reports, 2015, 5: 15058.
- [11] Lee Y S, Moon H S. Atomic coherence effects in four-wave mixing process of a ladder-type atomic system[J]. Optics Express, 2016, 24(10): 10723-10732.
- [12] Liu Z Y, Xiao J T, Lin J K, *et al.* High-efficiency backward four-wave mixing by quantum interference [J]. Scientific Reports, 2017, 7: 15796.
- [13] Zhang H J, Li X M, Sun D, *et al.* Phase control of highly efficient four-wave mixing in a six-level tripod atomic system [J]. Applied Optics, 2018, 57(3): 567-572.
- [14] Walker G, Arnold A S, Franke-Arnold S. Trans-spectral orbital angular momentum transfer via four-wave mixing in Rb vapor [J]. Physical Review Letters, 2012, 108(24): 243601.
- [15] Ding D S, Dong M X, Zhang W, *et al.* Experimental demonstration of quantum wrenching orbital angular momentum memory [EB/OL]. (2018-06-27) [2018-11-05]. <https://arxiv.org/abs/1806.10407>.
- [16] Akulshin A M, Novikova I, Mikhailov E E, *et al.* Arithmetic with optical topological charges in stepwise-excited Rb vapor [J]. Optics Letters, 2016, 41(6): 1146-1149.
- [17] Chopinaud A, Jacquy M, de Leseigno B V, *et al.* High helicity vortex conversion in a rubidium vapor [J]. Physical Review A, 2018, 97(6): 063806.
- [18] Ripka F, Kübler H, Löw R, *et al.* A room-temperature single-photon source based on strongly interacting Rydberg atoms [J]. Science, 2018, 362(6413): 446-449.
- [19] Ma R, Liu W, Qin Z Z, *et al.* Generating quantum correlated twin beams by four-wave mixing in hot cesium vapor [J]. Physical Review A, 2017, 96(4): 043843.
- [20] Wang L, Jing J T. Theoretical research on optimization of signal-noise ratio based on cascaded four-wave mixing system [J]. Acta Optica Sinica, 2017, 37(7): 0719001.
- 王丽, 荆杰泰. 基于级联四波混频系统实现信噪比优化的理论研究 [J]. 光学学报, 2017, 37(7): 0719001.
- [21] Yudin V I, Taichenachev A V, Basalaev M Y. Dynamic steady state of periodically driven quantum systems [J]. Physical Review A, 2016, 93(1): 013820.